Dinuclear Copper(II) and Cobalt(II) Complexes of the Tetradentate Ligand 1,2,4,5-Tetrakis(benzimidazol-2-yl)benzene (BTBI): Metallacyclic and Nonmetallacyclic Derivatives. X-ray Crystal Structures of $[Cu_2(BTBI)_2Cl_2][Cu_2(BTBI)Cl_2(DMF)_4]Cl_4 \cdot 12DMF$ and $[Co_2(BTBI)Br_4] \cdot 4DMF$

Santokh S. Tandon,[1a] Laurence K. Thompson,*[,1a] John N. Bridson,[1a] and John C. Dewan[1b]

Departments of Chemistry, Memorial University of Newfoundland, St. John's, Newfoundland, Canada A1B 3X7, and New York University, New York, New York 10003

Received July 8, 1993®

BTBI (1,2,4,5-tetrakis(benzimidazol-2-yl)benzene) acts as a tetradentate, dinucleating ligand, and on reaction with copper(II) salts forms both 2:1 (metal:ligand) and 2:2 derivatives, depending on reaction conditions. Initial reactions between BTBI and a large excess of copper salts produce "open" 2:1 derivatives, which rearrange on recrystallization and disproportionate to form 2:2 "closed" metallacyclic complexes or, with copper halides, species containing both types of cations. For example, the complex $[Cu_2(BTBI)Cl_4(DMF)_2 \cdot DMF \cdot H_2O$ (**I**) produces $[Cu_2(BTBI)_2Cl_2] \cdot [Cu_2(BTBI)Cl_2(DMF)Cl_4 \cdot 12DMF$ (**II**) on recrystallization from DMF/EtOH. With cobalt salts (CoX_2; X = Cl, Br, NCS) "open" 2:1 species are formed as the major products: $[Co_2(BTBI)X_4] \cdot 2DMF \cdot nH_2O$ (X = Cl, n = 0.5 (**X**); X = Br, n = 0 (**XI**); X = NCS, n = 3 (**XII**)). The crystal and molecular structures of compounds **II** and **XI** are reported. **II** crystallized in the triclinic system, space group $P\bar{1}$, with a = 15.538(4) Å, b = 17.044(2) Å, c = 15.186(4) Å, α = 92.11(2)°, β = 98.13(2)°, γ = 92.06(2)°, V = 3975(2) Å^3, and Z = 2. Refinement by full-matrix least-squares procedures gave final residuals of R = 0.066 and R_w = 0.063. Two square-pyramidal copper(II) centers are separated by 8.082(3) Å in the 2:2 centrosymmetric "closed" metallacyclic cation and by 8.805(3) Å in the 2:1 centrosymmetric "open" cation, which involves two coordinated DMF molecules per metal center. **XI** crystallized in the monoclinic system, space group $P2_1/n$, with a = 10.021(2) Å, b = 25.569(4) Å, c = 11.518(2) Å, β = 111.78(1)°, V = 2700.4(9) Å^3, and Z = 2. Refinement by full-matrix least-squares techniques gave final residuals of R = 0.066 and R_w = 0.072. Compound **XI** is centrosymmetric with the two tetrahedral cobalt(II) centers separated by 8.652(3) Å and the DMF molecules hydrogen-bonded to the NH- benzimidazole moieties. The spectral and magnetic properties of these complexes are also discussed. Very weak antiferromagnetic exchange exists in most of these complexes.

Introduction

In previous reports we decribed[2-5] the synthesis of the tetradentate, dinucleating ligand BTIM (1,2,4,5-tetrakis(4,5-dihydroimidazol-2-yl)benzene) and complexation with copper(II) and cobalt(II) salts. With copper(II) salts, BTIM forms dinuclear complexes of 2:2 stoichiometry having "closed" metallacyclic structures.[2,3,5] With cobalt(II) salts, complexes of both 2:2 and 2:1 (metal:ligand) stoichiometries possessing metallacyclic and nonmetallacyclic structures have been characterized.[4] The structures of the 2:2 metallacyclic derivatives involve two essentially parallel ligands bridging the two metal centers, creating a large unoccupied cavity with large metal–metal separations (>7.3 Å).[2,3,5] The 2:1 complexes involve open-chain, dinuclear structures with the two tetrahedral cobalt(II) centers bridged by one BTIM ligand, with a much larger metal–metal separation of 8.736(3) Å in the complex $[Co_2(BTIM)Cl_4] \cdot 2DMF$.[4] Despite many attempts, we could not characterize any copper(II) complexes of 2:1 stoichiometry. The large separation of the metal centers in these complexes, coupled with a ligand bridge with little tendency to propagate magnetic coupling, led to the presence of very weak exchange for both copper and cobalt complexes.

Our interest in the structural and magnetic properties of polynuclear metal complexes of multidentate, polynucleating macrocyclic[6-9] and noncyclic[10-12] ligands, in particular those in which the metal centers are separated by very large distances[11,12] and yet still exhibit significant spin coupling over these long molecular distances, led us to isolate the similar derivative BTBI (Figure 1), which contains larger peripheral donor groups (benzimidazoles), with aromatic character, a feature absent in BTIM. BTBI (1,2,4,5-tetrakis(benzimidazol-2-yl)benzene), like BTIM, is potentially a tetradentate, dinucleating ligand and on reaction with copper(II) salts forms both 2:1 and 2:2 derivatives and two complexes in which both 2:2 metallacyclic and 2:1 nonmetallacyclic species are present in the same compound. Only 2:1 cobalt complexes were isolated. In this report, the synthesis and structural, spectroscopic, and magnetic properties of copper(II) and cobalt(II) complexes of BTBI will be discussed.

Experimental Section

Synthesis of the Ligand (BTBI) and Its Copper(II) and Cobalt(II) Complexes. (a) BTBI (1,2,4,5-tetrakis(benzimidazol-2-yl)benzene)).

* To whom correspondence should be addressed.

® Abstract published in *Advance ACS Abstracts,* December 1, 1993.

(1) (a) Memorial University. (b) New York University.
(2) Mandal, S. K.; Thompson, L. K.; Newlands, M. J.; Gabe, E. J.; Lee, F. L. *J. Chem. Soc., Chem. Commun.* **1989**, 744.
(3) Mandal, S. K.; Thompson, L. K.; Newlands, M. J.; Gabe, E. J.; Lee, F. L. *Inorg. Chem.* **1990**, *29*, 3556.
(4) Tandon, S. S.; Thompson, L. K.; Bridson, J. N.; Dewan, J. C. *Can. J. Chem.* **1992**, *70*, 2771.
(5) McCarthy, C. J.; Thompson, L. K.; Newlands, M. J.; Hynes, R. C. *Acta Crystallogr.* **1992**, *C48*, 430.
(6) Tandon, S. S.; Thompson, L. K.; Bridson, J. N. *Inorg. Chem.* **1993**, *32*, 32.
(7) Tandon, S. S.; Thompson, L. K.; Bridson, J. N. *Inorg. Chem.* **1992**, *31*, 4635.
(8) Tandon, S. S.; Thompson, L. K.; Bridson, J. N. *J. Chem. Soc., Chem. Commun.* **1992**, 912.
(9) Tandon, S. S.; Thompson, L. K.; Bridson, J. N.; Bubenik, M. *Inorg. Chem.* **1993**, *32*, 4621.
(10) Tandon, S. S.; Mandal, S. K.; Thompson, L. K.; Hynes, R. C. *Inorg. Chem.* **1992**, *31*, 2215.
(11) Tandon, S. S.; Thompson, L. K.; Hynes, R. C. *Inorg. Chem.* **1992**, *31*, 2210.
(12) Tandon, S. S.; Mandal, S. K.; Thompson, L. K.; Hynes, R. C. *J. Chem. Soc., Chem. Commun.* **1991**, 1573.

0020-1669/94/1333-0054$04.50/0

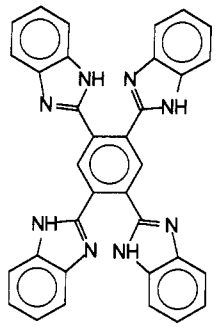

Figure 1. Structure of the ligand BTBI.

1,2,4,5-Tetracyanobenzene[13] (3.6 g, 20.2 mmol) and 1,2-diaminobenzene (9.0 g, 83.3 mmol) were added to polyphosphoric acid (50 mL), and the mixture was stirred at 180–190 °C for 4 h. The resulting dark brown solution was allowed to cool to 100 °C and poured into ice with vigorous stirring. A light brown solid formed, which was filtered off and stirred with a saturated solution of sodium bicarbonate for 1 h. It was then filtered off, washed with hot water (3 × 50 mL), acetone (3 × 50 mL), and finally ether (3 × 50 mL), and dried under vacuum. It is insoluble in most organic solvents and was used without further purification (yield 10.5 g, 95%). Mass spectrum (FABS), *m/e* (relative intensity): 543 (P + 1; 100), 452 (36), 438 (15), 427 (29), 425 (18), 361 (10), 338 (14), 155 (10), 143 (18), 119 (27), 102 (12), 92 (66). Mp: >320 °C.

(b) $[Cu_2(BTBI)Cl_4(DMF)_2]\cdot DMF\cdot H_2O$ (I), $[Cu_2(BTBI)(DMF)_2(H_2O)_2Br_2][CuBr_4]\cdot 2H_2O$ (III), $[Cu_2(BTBI)(DMF)_2(NO_3)_4]\cdot 2DMF\cdot 3H_2O$ (V), $[Cu_2(BTBI)(DMF)_3(H_2O)_3](BF_4)_4\cdot DMF$ (VI), $[Cu_2(BTBI)(DMF)_2(CF_3SO_3)_4]\cdot 2DMF\cdot 2H_2O$ (VIII). BTBI (0.54 g, 1 mmol) was added to a solution of $CuCl_2\cdot 2H_2O$ (1.02 g, 6 mmol) in DMF (50 mL). The reaction mixture was stirred at room temperature for 1 h; during this period the ligand dissolved, resulting in the formation of a green solution. The resulting solution was filtered, and the filtrate was concentrated to 5–10 mL on a rotary evaporator at 75–80 °C. Ethanol (15 mL) was added to the concentrated solution of the complex, while hot, and the resulting mixture allowed to stand at room temperature overnight. A dark green crystalline compound formed, which was filtered off, washed with a 1:1DMF:EtOH mixture (3 × 5 mL), and dried under vacuum (yield 70%). Anal. Calcd for $[Cu_2(C_{34}H_{22}N_8)Cl_4(DMF)_2]\cdot DMF\cdot H_2O$ (I): C, 49.24; H, 4.31; N, 14.69; Cu, 12.11. Found: C, 49.04; H, 3.76; N, 14.10; Cu, 11.80. Recrystallization from a DMF/EtOH mixture produced bright green crystals of **II** suitable for X-ray diffraction studies. Anal. Calcd for $[Cu_2(C_{34}H_{22}N_8)_2Cl_2][Cu_2(C_{34}H_{22}N_8)Cl_2(DMF)_4]Cl_4\cdot 12DMF$ (II): C, 54.01; H, 5.35; N, 16.80; Cu, 7.62. Found: C, 53.82; H, 5.18; N, 17.07; Cu, 8.20. The 2:1 compounds **III**, **V**, **VI**, and **VIII** were prepared in a similar manner by reacting BTBI with a large excess of the copper(II) salts ($CuX_2\cdot nH_2O$; X = Br (**III**), NO_3 (**V**), BF_4 (**VI**), CF_3SO_3 (**VIII**)). Concentration of DMF solutions and addition of ethanol produced nice blue-green crystals of **V**, **VI**, and **VIII** and brown crystals of **III**, suitable for X-ray analysis, but unfortunately they decompose when exposed to the X-ray beam. (Yields: 60–70%.) Anal. Calcd for $[Cu_2(C_{34}H_{22}N_8)(DMF)_2(H_2O)_2Br_2][CuBr_4]\cdot 2H_2O$ (III): C, 33.55; H, 3.08; N, 9.79; Cu, 13.32. Found: C, 33.32; H, 2.99; N, 10.06; Cu, 12.88. Anal. Calcd for $[Cu_2(C_{34}H_{22}N_8)(NO_3)_4(DMF)_2]\cdot 2DMF\cdot 3H_2O$ (V): C, 40.50; H, 4.11; N, 12.33; Cu, 9.32. Found: C, 40.08; H, 4.21; N, 12.51; Cu, 9.05. Anal. Calcd for $[Cu_2(C_{34}H_{22}N_8)(DMF)_3(H_2O)_3](BF_4)_4\cdot DMF$ (VI): C, 43.71; H, 4.43; N, 17.74; Cu, 10.06. Found: C, 43.44; H, 4.33; N, 17.95; Cu, 9.54. Anal. Calcd for $[Cu_2(C_{34}H_{22}N_8)(DMF)_2(CF_3SO_3)_4]\cdot 2DMF\cdot 2H_2O$ (VIII): C, 37.67; H, 3.40; N, 10.54; Cu, 7.97. Found: C, 37.65; H, 3.27; N, 10.97; Cu, 7.68.

Recrystallization of **III** from DMF gave a greenish-brown crystalline compound which corresponds to $[Cu_2(BTBI)Br_4(DMF)_2]$ (Anal. Calcd: Cu, 11.19. Found: Cu, 10.86). Recrystallization of this compound from hot DMF gave a bright green crystalline compound **IV**. Anal. Calcd for $[Cu_2(C_{34}H_{22}N_8)_2Br_2][Cu_2(BTBI)Br_2(DMF)_4]Br_4\cdot 6DMF\cdot 4H_2O$ (IV): C, 47.67; H, 4.35; N, 14.32. Found: C, 47.51; H, 3.72; N, 13.79. Recrystallization of **VI** from DMF/EtOH gave green-blue crystals of **VII**. Anal. Calcd for $[Cu_2(C_{34}H_{22}N_8)_2(DMF)_2](BF_4)_4\cdot 2DMF\cdot 2H_2O$ (VII): C, 50.87; H, 4.04; N, 14.83. Found: C, 50.44; H, 4.22; N, 14.91. Recrystallization of **VIII** from DMF/EtOH gave a green-blue crystalline compound **IX**. Anal. Calcd for $[Cu_2(C_{34}H_{22}N_8)_2(DMF)_2](CF_3SO_3)_4\cdot DMF\cdot 5H_2O$ (IX): C, 45.94; H, 3.56; N, 12.57. Found: C, 45.68; H, 3.14; N, 12.13.

(c) $[Co_2(BTBI)X_4]\cdot 2DMF\cdot nH_2O$ (X = Cl, n = 0.5 (X); X = Br, n = 0 (XI); X = NCS, n = 3 (XII)). CoX_2 (X = Cl (1.42 g, 6 mmol); X = Br (1.96 g, 6 mmol)) was dissolved in DMF (100 mL). BTBI (0.540 g, 1 mmol) was added and the mixture heated on a steam bath for 20 h, during which time most of the ligand dissolved, forming a deep blue solution. The solution was filtered and the filtrate concentrated to ca. 5 mL under reduced pressure. Blue crystals suitable for X-ray analysis were obtained on standing; these were filtered off, washed with ethanol (3 × 5 mL), and dried under vacuum. More complex was obtained after adding ethanol to the mother liquor (yields 70% (**X**), 80% (**XI**)). Anal. Calcd for $[Co_2(C_{34}H_{22}N_8)Cl_4]\cdot 2DMF\cdot 0.5H_2O$ (X): C, 50.17; H, 3.87; N, 14.63; Co, 12.31. Found: C, 49.92; H, 3.98; N, 14.60; Co, 12.12. Anal. Calcd for $[Co_2(C_{34}H_{22}N_8)Br_4]\cdot 2DMF$ (XI). C, 42.64; H, 3.20; N, 12.44; Co, 10.46. Found: C, 42.95; H, 2.99; N, 12.05; Co, 10.39. The crystals of **XI** used for X-ray analysis contain four DMF molecules. $[Co_2(BTBI)(NCS)_4]\cdot 2DMF\cdot 3H_2O$ (**XII**) was prepared in a similar manner by reacting BTBI (0.54 g, 1 mmol) with cobalt(II) thiocyanate (6 mmol) (prepared in situ by reaction of cobalt(II) nitrate with potassium thiocyanate and filtration of insoluble potassium nitrate) at room temperature for 1 h and was obtained as a blue solid (yield 75%). Anal. Calcd for $[Co_2(C_{34}H_{22}N_8)(NCS)_4]\cdot 2DMF\cdot 3H_2O$ (XII): C, 48.36; H, 3.85; N, 17.95; Co, 10.79. Found: C, 48.45; H, 3.47; N, 17.53; Co, 11.00.

Physical Measurements. The FABS mass spectrum was obtained for a glycerol mull by using a VG Micromass 7070 HS spectrometer with a direct insertion probe. Electronic spectra were recorded for mulls and DMF solutions using a Cary 5E spectrometer. Infrared spectra were recorded for Nujol mulls using a Mattson Polaris FT-IR instrument. ESR spectra were obtained using a Bruker ESP 300 X-band spectrometer at room temperature and 77 K. Microanalyses (C, H, N) were carried out by Canadian Microanalytical Service, Delta, Canada, and metal analyses were performed by EDTA titration. Room-temperature magnetic susceptibilities were measured by the Faraday method using a Cahn 7600 Faraday magnetic susceptibility system, and variable-temperature magnetic data (4–300 K) were obtained using an Oxford Instruments superconducting Faraday susceptometer with a Sartorius 4432 microbalance. A main solenoid field of 1.5 T and a gradient field of 10 T m^{-1} were employed.

Crystallographic Data Collection and Refinement of the Structures. (a) $[Cu_2(BTBI)_2Cl_2][Cu_2(BTBI)Cl_2(DMF)_4]Cl_4\cdot 12DMF$ (II). Crystals of II are green and have a regular polyhedral shape. The diffraction intensities of an approximately 0.400 × 0.250 × 0.200 mm crystal were collected with graphite-monochromatized Mo Kα radiation and a 2-kW sealed-type generator using a Rigaku AFC6S diffractometer at −100(1) °C with the ω–2θ scan technique to a $2\theta_{max}$ value of 40.0°. A total of 6017 reflections were collected, of which 5647 were unique and 4359 were considered significant with $I_{net} > 2.0\sigma(I_{net})$. The intensities of three representative reflections, which were measured after every 150 reflections, declined by 18%. A nonlinear correction factor was applied to the data to account for this phenomenon. The compound appears to decompose in the beam, even at low temperature, and does so in a nonlinear fashion,

Table 1. Crystallographic Data for $[Cu_2(BTBI)_2Cl_2][Cu_2(BTBI)Cl_2(DMF)_4)]Cl_4\cdot 12DMF$ (II) and $[Cl_2(BTBIBr_4]\cdot 4DMF$ (XI)

	II	XI
chem formula	$C_{72.9}H_{84.3}N_{19.3}Cu_2Cl_4O_{7.3}$	$Cu_{40}H_{50}Br_4Co_2N_{12}O_4$
fw	1616.4	1272.46
space group	$P\bar{1}$	$P2_1/n$
a (Å)	15.538(4)	10.021(2)
b (Å)	17.044(2)	25.569(4)
c (Å)	15.186(4)	11.518(2)
α (deg)	92.11(2)	
β (deg)	98.13(2)	111.78(1)
γ (deg)	92.06(2)	
V (Å^3)	3975(2)	2740.4(9)
Z	2	2
t (°C)	−100(1)	25
λ (Å)	0.710 69 (Mo Kα)	1.541 78 (Cu Kα)
ρ_{calc} (g·cm^{-3})	1.350	1.542
μ (cm^{-1})	7.33	88.49
R	0.066	0.066
R_w	0.063	0.072

[a] $R = \Sigma||F_o| - |F_c||/\Sigma|F_o|$; $R_w = [(\Sigma w(|F_o| - |F_o| - |F_c|)^2/\Sigma wF_o^2)]^{1/2}$.

(13) Bailey, A. S.; Henn, B. R.; Langdon, J. M. *Tetrahedron* **1963**, *19*, 161.

Table 2. Final Atomic Positional Parameters and B_{eq} Values for $[Cu_2(BTBI)_2Cl_2][Cu_2(BTBI)Cl_2(DMF)_4]Cl_4 \cdot 12DMF$ (II)

atom	x	y	z	B_{eq}[a] (Å^2)	atom	x	y	z	B_{eq}[a] (Å^2)
Cu(1)	0.0515(1)	−0.22216(7)	−0.07183(8)	1.95(7)	C(23)	−0.0444(7)	0.1327(6)	0.3321(7)	1.9(2)
Cu(2)	0.4138(1)	0.28964(7)	0.62866(8)	1.92(8)	C(24)	−0.0620(7)	0.1360(6)	0.4198(7)	2.8(3)
Cl(1)	0.0843(2)	−0.3558(2)	−0.1115(2)	3.5(2)	C(25)	−0.1001(8)	0.2035(7)	0.4449(8)	3.5(3)
Cl(2)	0.4684(2)	0.1684(2)	0.6151(2)	3.5(2)	C(26)	−0.1206(8)	0.2638(7)	0.3872(8)	3.7(3)
Cl(3)	0.3713(2)	0.0770(2)	0.0856(2)	3.3(2)	C(27)	−0.1021(7)	0.2595(6)	0.2994(7)	2.9(3)
Cl(4)	0.9134(2)	0.0706(2)	0.6312(2)	3.3(2)	C(28)	−0.0650(7)	0.1911(6)	0.2735(7)	2.0(2)
O(1)	0.4041(6)	0.3153(4)	0.4859(5)	3.7(4)	C(29)	0.0725(7)	−0.0828(5)	0.0976(6)	1.4(2)
O(2)	0.2932(5)	0.2450(5)	0.6235(5)	2.9(4)	C(30)	0.1303(7)	−0.0535(5)	0.0417(6)	1.3(2)
O(3)	0.527(1)	0.514(1)	0.842(1)	10.8(5)	C(31)	0.1390(7)	0.0283(5)	0.0357(6)	1.5(2)
O(4)	0.2760(8)	0.1161(7)	0.3877(8)	10.4(4)	C(32)	0.0979(7)	0.0819(5)	0.0854(6)	1.3(2)
O(5)	0.219(1)	0.482(1)	0.371(1)	5.6(5)	C(33)	0.0406(7)	0.0518(5)	0.1404(6)	1.1(2)
O(5A)	0.249(1)	0.455(1)	0.334(1)	4.3(5)	C(34)	0.0269(7)	−0.0289(5)	0.1436(6)	1.5(2)
O(6)	0.181(1)	0.573(1)	0.485(1)	9.3(7)	C(35)	0.5674(9)	0.4004(6)	0.6417(7)	1.5(2)
O(7)	0.1791(7)	0.0442(6)	0.8252(7)	8.9(3)	C(36)	0.6652(8)	0.3625(6)	0.7470(7)	2.4(3)
O(8)	0.6568(6)	0.3230(6)	0.3909(7)	6.6(3)	C(37)	0.7394(8)	0.3520(7)	0.8094(8)	3.8(3)
N(1)	0.0545(5)	−0.2295(4)	0.0628(5)	1.6(2)	C(38)	0.734(1)	0.2912(8)	0.8673(9)	5.0(3)
N(2)	0.0594(5)	−0.1847(4)	0.2035(5)	1.9(2)	C(39)	0.657(1)	0.2425(7)	0.8618(8)	4.6(3)
N(3)	0.1738(5)	−0.1698(4)	−0.0453(5)	1.5(2)	C(40)	0.5851(8)	0.2528(6)	0.7979(8)	3.2(3)
N(4)	0.2731(6)	−0.0733(4)	−0.0034(5)	1.8(2)	C(41)	0.5918(8)	0.3137(6)	0.7400(7)	2.2(3)
N(5)	0.0818(5)	0.2282(5)	0.0851(5)	1.6(2)	C(42)	0.3845(7)	0.4615(6)	0.6257(7)	1.4(2)
N(6)	0.2116(6)	0.1825(5)	0.0802(5)	2.4(2)	C(43)	0.2893(7)	0.4883(6)	0.7146(7)	2.0(3)
N(7)	−0.0358(5)	0.1704(4)	0.1914(5)	1.8(2)	C(44)	0.2324(8)	0.5236(6)	0.7694(8)	3.2(3)
N(8)	−0.0047(5)	0.0758(4)	0.2871(5)	1.9(2)	C(45)	0.1950(8)	0.4740(7)	0.8245(8)	3.8(3)
N(9)	0.5302(5)	0.3396(4)	0.6739(5)	1.5(4)	C(46)	0.2128(8)	0.3941(6)	0.8286(7)	2.9(3)
N(10)	0.6495(6)	0.4166(5)	0.6823(6)	2.4(5)	C(47)	0.2667(7)	0.3606(6)	0.7749(7)	2.3(3)
N(11)	0.3651(6)	0.3932(4)	0.6599(5)	1.8(4)	C(48)	0.3057(8)	0.4089(6)	0.7177(7)	1.7(2)
N(12)	0.3386(6)	0.5208(5)	0.6567(6)	2.3(5)	C(49)	0.5299(7)	0.4507(5)	0.5691(6)	1.2(2)
N(13)	0.1885(9)	0.1479(6)	0.5969(7)	3.0(6)	C(50)	0.4447(7)	0.4769(5)	0.5613(6)	1.4(2)
N(14)	0.4209(9)	0.2794(6)	0.3457(7)	6.4(7)	C(51)	0.4172(7)	0.5264(5)	0.4917(7)	1.6(2)
N(15)	0.531(1)	0.415(1)	0.946(1)	7.4(4)	C(52)	0.265(1)	0.1799(9)	0.5903(9)	3.3(8)
N(16)	0.3246(8)	0.0061(6)	0.3272(7)	5.0(3)	C(53)	0.1585(9)	0.0697(8)	0.559(1)	6.5(9)
N(17)	0.154(2)	0.344(1)	0.327(2)	5.0(6)	C(54)	0.129(1)	0.1865(8)	0.646(1)	5.1(8)
N(17A)	0.165(2)	0.360(1)	0.387(2)	4.9(6)	C(55)	0.412(1)	0.2664(7)	0.429(1)	4.8(8)
N(18)	0.102(2)	0.475(2)	0.538(2)	7.7(7)	C(56)	0.433(1)	0.353(1)	0.3133(9)	10(1)
N(19)	0.316(1)	0.0559(8)	0.8089(9)	7.5(3)	C(57)	0.427(2)	0.214(1)	0.281(1)	13(1)
N(20)	0.6752(8)	0.2200(7)	0.472(1)	6.0(3)	C(58)	0.495(2)	0.457(2)	0.876(2)	10.7(7)
C(1)	0.0635(7)	−0.1655(6)	0.1184(7)	1.9(2)	C(59)	0.482(1)	0.355(1)	0.976(1)	7.5(5)
C(2)	0.0484(7)	−0.2652(6)	0.2044(7)	2.2(3)	C(60)	0.618(1)	0.425(1)	0.991(1)	8.3(6)
C(3)	0.0434(7)	−0.3149(6)	0.2752(7)	3.1(3)	C(61)	0.266(1)	0.058(1)	0.332(1)	8.5(5)
C(4)	0.0328(8)	−0.3937(7)	0.2524(8)	3.7(3)	C(62)	0.311(1)	−0.0564(8)	0.260(1)	6.8(4)
C(5)	0.0274(7)	−0.4232(6)	0.1659(8)	3.1(3)	C(63)	0.405(1)	0.015(1)	0.384(1)	11.5(6)
C(6)	0.0338(7)	−0.3745(6)	0.0951(7)	2.5(3)	C(64)	0.216(2)	0.395(2)	0.348(2)	15.1(9)
C(7)	0.0438(7)	−0.2935(6)	0.1166(7)	1.7(2)	C(65)	0.082(2)	0.390(1)	0.308(2)	5.0(7)
C(8)	0.1899(7)	−0.1002(6)	−0.0032(6)	1.5(2)	C(65A)	0.180(2)	0.374(2)	0.485(3)	9(1)
C(9)	0.3138(8)	−0.1276(6)	−0.0502(7)	2.0(2)	C(66)	0.148(2)	0.269(1)	0.338(2)	3.4(6)
C(10)	0.3996(8)	−0.1285(6)	−0.0663(7)	2.8(3)	C(66A)	0.145(3)	0.278(3)	0.398(3)	13(2)
C(11)	0.4215(8)	−0.1942(7)	−0.1117(8)	3.8(3)	C(67)	0.178(2)	0.505(2)	0.508(2)	9(1)
C(12)	0.361(1)	−0.2555(7)	−0.1401(8)	4.3(3)	C(68)	0.107(2)	0.394(2)	0.566(2)	8(1)
C(13)	0.2740(8)	−0.2545(6)	−0.1229(7)	2.9(3)	C(69)	0.035(2)	0.524(2)	0.541(2)	10(1)
C(14)	0.2517(7)	−0.1889(6)	−0.0765(7)	1.9(2)	C(70)	0.245(1)	0.010(1)	0.798(1)	9.9(6)
C(15)	0.1275(8)	0.1641(6)	0.0842(6)	1.8(2)	C(71)	0.396(2)	0.024(1)	0.786(1)	14.4(7)
C(16)	0.2208(8)	0.2621(6)	0.0793(7)	2.6(3)	C(72)	0.328(1)	0.131(1)	0.845(1)	11.6(6)
C(17)	0.2962(8)	0.3114(7)	0.0806(8)	3.9(3)	C(73)	0.671(2)	0.253(2)	0.398(2)	4.6(8)
C(18)	0.283(1)	0.3915(8)	0.0830(8)	4.8(3)	C(73A)	0.681(1)	0.310(1)	0.459(2)	4.8(6)
C(19)	0.2010(9)	0.4205(7)	0.0854(8)	3.9(3)	C(74)	0.701(1)	0.223(1)	0.563(1)	10.1(5)
C(20)	0.1273(8)	0.3727(7)	0.0855(7)	3.0(3)	C(75)	0.682(3)	0.127(3)	0.457(3)	8(1)
C(21)	0.1402(8)	0.2923(6)	0.0837(7)	2.1(3)	C(75A)	0.641(2)	0.163(2)	0.417(2)	9(1)
C(22)	−0.0008(7)	0.1017(6)	0.2037(7)	1.7(2)					

[a] $B_{eq} = (8\pi^2/3)\sum_{i=1}^{3}\sum_{j=1}^{3} U_{ij} \mathbf{a}_i^* \mathbf{a}_j^* \mathbf{\hat{a}}_i \cdot \mathbf{\hat{a}}_j$.

exhibiting a more rapid intensity loss in the middle of the collection. Two similar scaling factors were refined, and a third-order polymonial was used to model the decay. The data collection was stopped just before completion of the second shell, when an increased intensity loss occurred. The data set contains all but a few reflections out to $2\theta = 40°$. An empirical absorption correction was applied using the program DIFABS,[14] which resulted in transmission factors ranging from 0.97 to 1.04. The data were corrected for Lorentz and polarization effects, and the cell parameters were obtained from the least-squares refinement of the setting angles of 24 carefully centered reflections with 2θ in the range 8.59–26.70°.

The structure was solved by direct methods.[15,16] Only the copper and chlorine atoms, oxygens O(1) and O(2), nitrogens N(9)–N(14), and carbons C(52)–C(57) were refined anisotropically. The hydrogen atoms were placed in calculated postitions, and their B values were fixed at 1.2 times the B_{eq} of the atom to which they were bound. They were included, but not refined in the final least-squares cycles. The final cycle of full-matrix least-squares refinement was based on 4359 observed reflections ($I > 2.00\sigma(I)$) and 563 variable parameters and converged with unweighted and weighted agreement factors of $R = \sum||F_o| - |F_c||/\sum|F_o| = 0.066$ and $R_w = [(\sum w(|F_o| - |F_c|)^2/\sum wF_o^2)]^{1/2} = 0.063$. The maximum and minimum peaks on the final difference Fourier map corresponded to 0.84 and −0.49 electron/Å^3, respectively. Neutral-atom scattering factors[17] and anom-

(14) Walker, N.; Stuart, D. *Acta Crystallogr.* **1983**, *A39*, 158.
(15) Gilmore, C. J. *J. Appl. Crystallogr.* **1984**, *17*, 42.
(16) Beurskens, P. T. DIRDIF, Technical Report 1984/1; Crystallography Laboratory: Toernooiveld, 6525 Ed Nijmegen, The Netherlands, 1984.
(17) Cromer, D. T.; Waber, J. T. *International Tables for X-ray Crystallography*; The Kynoch Press: Birmingham, U.K., 1974; Vol. IV, Table 2.2A.

alous-dispersion terms[18,19] were taken from the usual sources. All calculations were performed with the TEXSAN[20] crystallographic software package using a VAX 3100 work station. A summary of the crystal and other data is given in Table 1 (full details are given in supplementary Table SI), and atomic coordinates are given in Table 2. Hydrogen atom atomic coordinates (Table SII), anisotropic thermal parameters (Table SIII), complete bond lengths and angles (Table SIV), and least-squares planes data (Table SV) are included as supplementary material.

(b) $[Co_2(BTBI)Br_4]\cdot 4DMF$ (XI). The diffraction intensities of a blue-green block-shaped crystal of approximate dimensions 0.250 × 0.140 × 0.090 mm were collected with Ni-filtered Cu Kα radiation and a 12-kW rotating anode generator running at 9 kW using a Rigaku AFC6R diffractometer at 25 ± 1 °C and the ω–2θ scan technique to a $2\theta_{max}$ value of 120.0°. Cell constants were obtained by the least-squares refinement of the setting angles of 25 carefully centered reflections with 2θ in the range 33.09–34.88°. A total of 4455 reflections were collected, of which 4190 were unique (R_{int} = 0.036) and 2894 were considered significant with $I_{net} > 2.00\sigma(I_{net})$. The intensities of three representative reflections, which were measured after every 500 reflections, remained constant throughout data collection, indicating crystal and electronic stability. An empirical absorption correction was applied, after a full isotropic refinement, using the program DIFABS,[14] which resulted in transmission factors ranging from 0.52 to 1.77. The data were corrected for Lorentz and polarization effects, and the structure was solved by direct methods.[15,16] The non-hydrogen atoms were refined anisotropically. H atoms were placed in calculated positions, and their B values were fixed at 1.2 times the B_{eq} of the atom to which they were bound. The final cycle of full-matrix least-squares refinement was based on 2894 observed reflections ($I > 2.00\sigma(I)$) and 316 variable parameters and converged with unweighted and weighted agreement factors of R = 0.066 and R_w = 0.072. The maximum and minimum peaks on the final difference Fourier map corresponded to 0.39 and –0.70 electron/Å^3, respectively. Neutral-atom scattering factors[17] and anomalous-dispersion terms[18,19] were taken from the usual sources. All calculations were performed with the TEXSAN[20] crystallographic software package. A summary of the crystal and other data is given in Table I (full details are given in supplementary Table SI), and atomic coordinates are given in Table 3. Hydrogen atom coordinates (Table SVI), anisotropic thermal parameters (Table SVII), complete bond lengths and angles (Table SVIII), and least-squares planes data (Table SIX) are included as supplementary material.

Results and Discussion

Although BTBI is insoluble in almost all organic solvents tried so far, it reacts successfully with metal salts in DMF solutions to form soluble complexes, which are obtained as crystalline solids by the concentration of the solutions to very small volumes or in some cases by the addition of ethanol. Most of these complexes contain DMF molecules, which are coordinated to the metal centers in some cases. The complexes or their DMF solutions, on treatment with water, undergo rapid decomplexation, indicating a fairly weak coordinating ability for this ligand in the presence of water. This may be attributed, in part, to the formation of a seven-membered chelate ring involving the two adjacent benzimidazole groups. By comparison the complexes of BTIM were much more stable under these circumstances.[3,4]

In the initial reactions for the preparation of complexes **I**, **III**, **V**, **VI**, and **VIII**, in which a large excess of metal salt was reacted with BTBI in DMF, 2:1 derivatives were produced. The stabilization of these species is clearly due to the presence of excess metal ion, which is also responsible for the inclusion of the $CuBr_4^{2-}$ anion in **III**. A similar chloro complex was not observed. Recrystallization in DMF causes disproportionation in all cases, with the formation of complexes containing metallacyclic 2:2 species. The bromide complex **III** produces the simple 2:1 species, corresponding to **I**, in the first recrystallization step and then on further recrystallization forms the mixed 2:2/2:1 species **IV**, which corresponds to the analogous chloro complex **II**.

Table 3. Final Atomic Positional Parameters and B_{eq} Values for $[Co_2(BTBI)Br_4]\cdot 4DMF$ (**XI**)

atom	x	y	z	B_{eq}[a] (Å^2)
Br(1)	0.6743(1)	0.22255(4)	0.0503(1)	7.63(5)
Br(2)	1.0476(1)	0.14985(4)	0.1491(1)	7.93(6)
Co	0.7971(1)	0.14517(5)	0.0363(1)	5.21(6)
O(21)	0.840(1)	–0.0141(3)	–0.4050(9)	10.7(5)
O(31)	0.783(1)	–0.1071(3)	0.1790(9)	10.1(4)
N(1)	0.7156(6)	0.0791(2)	0.0791(7)	4.9(3)
N(2)	0.7048(7)	–0.0051(2)	0.1216(7)	5.1(3)
N(3)	0.7563(7)	0.1202(2)	–0.1385(6)	4.7(3)
N(4)	0.7720(7)	0.0679(2)	–0.2863(7)	5.3(3)
N(21)	0.910(1)	–0.0877(3)	–0.459(1)	8.1(5)
N(31)	0.807(1)	–0.1927(3)	0.1470(8)	7.3(4)
C(1)	0.7672(8)	0.0320(3)	0.0758(8)	4.8(3)
C(2)	0.6049(8)	0.0199(3)	0.1572(8)	5.1(4)
C(3)	0.509(1)	–0.0002(3)	0.210(1)	6.2(4)
C(4)	0.419(1)	0.0371(4)	0.231(1)	6.8(5)
C(5)	0.421(1)	0.0891(4)	0.200(1)	6.5(5)
C(6)	0.5176(8)	0.1081(3)	0.1517(9)	5.6(4)
C(7)	0.6101(8)	0.0719(3)	0.1299(8)	4.9(3)
C(8)	0.8087(8)	0.0763(3)	–0.1630(8)	4.7(4)
C(9)	0.686(1)	0.1090(3)	–0.348(1)	5.5(4)
C(10)	0.614(1)	0.1200(4)	–0.476(1)	6.7(5)
C(11)	0.536(1)	0.1657(4)	–0.506(1)	7.4(5)
C(12)	0.530(1)	0.1994(4)	–0.413(1)	7.4(5)
C(13)	0.599(1)	0.1886(3)	–0.286(1)	6.2(4)
C(14)	0.6784(8)	0.1424(3)	–0.2556(9)	5.1(3)
C(15)	0.8849(8)	0.0178(3)	0.0323(9)	5.0(3)
C(16)	0.9035(8)	0.0386(3)	–0.0740(8)	4.6(3)
C(17)	0.9811(8)	–0.0198(3)	0.1020(8)	4.9(3)
C(21)	1.048(2)	–0.104(1)	–0.439(2)	24(2)
C(22)	0.826(3)	–0.131(1)	–0.507(2)	24(2)
C(23A)	0.816(4)	–0.057(1)	–0.448(3)	10(2)
C(23B)	0.935(3)	–0.043(1)	–0.404(3)	9(1)
C(31)	0.964(1)	–0.1930(5)	0.199(1)	10.2(7)
C(32)	0.736(1)	–0.2426(5)	0.097(2)	11.3(7)
C(33)	0.733(2)	–0.1509(5)	0.143(1)	9.6(7)

[a] $B_{eq} = (8\pi^2/3)\sum_{i=1}^{3}\sum_{j=1}^{3} U_{ij}\mathbf{a}_i^*\mathbf{a}_j^*\mathbf{a}_i\mathbf{a}_j$.

The role of the anion as a ligand is clearly important in stabilizing the 2:1 species, in particular because the ligand only provides two nitrogen donors per metal center, and it is of interest to note that this species persists in **II** and **IV**. For species involving weakly coordinating anions, no mixed-stoichiometry complexes have been found and recrystallization produces just the 2:2 species. In the absence of extra metal, and reasonable anionic ligands, the 2:2 metallacyclic species appear to be the most stable. In the case of BTIM, no examples of 2:1 complexes were isolated, and its copper coordination chemistry was dominated by the formation of 2:2 metallacyclic species.[2,3,5]

For cobalt(II), blue (**X**, **XII**) and blue-green (**XI**) 2:1 complexes were formed with halide anions, which have a reasonable affinity for cobalt(II), and on recrystallization these species did not undergo significant decomposition. However, for anions with relatively weak coordinating ability, e.g. NO_3 and ClO_4, the formation of 2:2 metallacyclic species is the norm.[21]

Description of the Structure of $[Cu_2(BTBI)_2Cl_2][Cu_2(BTBI)Cl_2(DMF)_4]Cl_4\cdot 12DMF$ (II). The structure of **II** is quite complicated, with nine fragments in the asymmetric unit, including half the 2:2 centrosymmetric unit, half the 2:1 centrosymmetric unit, two chloride ions, a DMF at 0.8 occupancy, three fully occupied DMF molecules with one disordered over two orientations, and a DMF pair, with one molecule disordered over two orientations with 0.5 occupancy in each and the second with 0.5 occupancy. Some DMF molecules appear to be hydrogen-bonded to the noncoordinated benzimidazole NH group.

The 2:2 metallacyclic fragment is illustrated in Figure 2, and bond lengths and angles relevant to the copper coordination spheres are given in Table 4. Two square-pyramidal copper(II) centers, each bonded by four equatorial benzimidazole nitrogens (Cu–N

(18) Ibers, J. A.; Hamilton, W. C. *Acta Crystallogr.* **1974**, *17*, 781.
(19) Cromer, D. T. *International Tables for X-ray Crystallography*; The Kynoch Press: Birmingham, U.K., 1974; Vol. IV, Table 2.3.1.
(20) *Texsan-Texray Structure Analysis Package*; Molecular Structure Corp.: The Woodlands, TX, 1985.
(21) Tandon, S. S.; Thompson, L. K. Unpublished results.

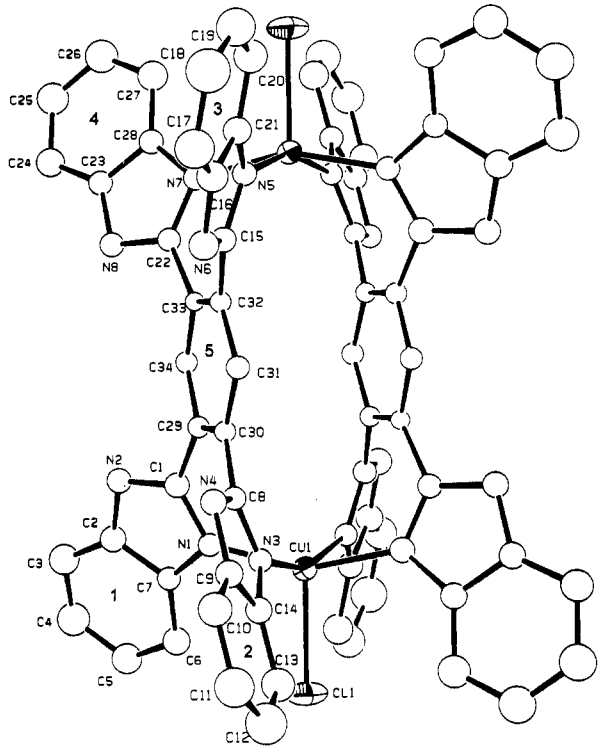

Figure 2. Perspective view of 2:2 metallacyclic cation $[Cu_2(BTBI)_2Cl_2]^{2+}$ in **II**.

Table 4. Intramolecular Distances (Å) and Angles (deg) Relevant to Copper Coordination Spheres in $[Cu_2(BTBI)_2Cl_2][Cu_2(BTBI)Cl_2(DMF)_4]Cl_4 \cdot 12DMF$ (**II**)

Cu(1)–Cl(1)	2.425(3)	Cu(1)–N(1)	2.047(8)
Cu(1)–N(3)	2.050(8)	Cu(1)–N(5)	2.051(9)
Cu(1)–N(7)	2.036(8)	Cu(2)–Cl(2)	2.275(3)
Cu(2)–O(1)	2.212(8)	Cu(2)–O(2)	1.986(8)
Cu(2)–N(9)	1.992(8)	Cu(2)–N(11)	2.011(8)
Cl(1)–Cu(1)–N(1)	100.3(2)	Cl(1)–Cu(1)–N(3)	101.4(2)
Cl(1)–Cu(1)–N(5)	102.2(2)	Cl(1)–Cu(1)–N(7)	102.9(2)
N(1)–Cu(1)–N(3)	87.4(3)	N(1)–Cu(1)–N(5)	88.6(3)
N(1)–Cu(1)–N(7)	156.8(3)	N(3)–Cu(1)–N(5)	156.5(3)
N(3)–Cu(1)–N(7)	88.8(3)	N(5)–Cu(1)–N(7)	85.8(3)
Cl(2)–Cu(2)–O(1)	95.9(2)	Cl(2)–Cu(2)–O(2)	92.2(2)
Cl(2)–Cu(2)–N(9)	92.9(2)	Cl(2)–Cu(2)–N(11)	171.4(2)
O(1)–Cu(2)–O(2)	96.4(3)	O(1)–Cu(2)–N(9)	100.3(3)
O(1)–Cu(2)–N(11)	92.7(3)	O(2)–Cu(2)–N(9)	161.9(3)
O(2)–Cu(2)–N(11)	86.2(3)	N(9)–Cu(2)–N(11)	86.2(3)
Cu(2)–O(1)–C(55)	123.4(8)	Cu(2)–O(2)–C(52)	127(1)

= 2.036(8), 2.050(8) Å), and an axial chlorine (Cu(1)–Cl(1) = 2.425(3) Å), are bridged in the familiar, centrosymmetric, metallacyclic arrangement in which the two metals and the two ligands create a large empty cavity with the central benzene rings eclipsed and coplanar. The metal centers are separated by 8.082(3) Å, and the parallel benzene rings, by 3.529(9) Å. The overall dimensions of the metallacycle are similar to those reported for $[Cu_2(BTIM)_2Cl_2]^{2+}$.[3] Benzimidazole rings 1 and 2 are mutually twisted by 70.8° and twisted by 41.8 and 39.2°, respectively, relative to the central benzene ring (5). Benzimidazole rings 3 and 4 are mutually twisted by 71.0° and twisted by 38.9 and 39.4°, respectively, relative to the central benzene ring. The copper atoms are displaced by 0.414(8) Å from the mean N_4 basal plane toward the apical chlorine.

The structure of the 2:1 open-chain fragment, $[Cu_2(BTBI)(DMF)_4Cl_2]^{2+}$, is illustrated in Figure 3. The cation is centrosymmetric with the center of inversion coincident with the center of the central benzene ring. Each copper atom adopts a square-pyramidal geometry with two benzimidazole nitrogens, a chlorine and a DMF bound in the equatorial plane, and an axial DMF. Copper–nitrogen distances (1.992(8), 2.011(8) Å) compare closely with those in the 2:2 fragment. The equatorial copper–oxygen (DMF) distance (1.986(8) Å) is substantially shorter than the axial DMF contact (2.212(8) Å), and the equatorial Cu–Cl distance (2.275(3) Å) is much shorter than the axial distance in the 2:2 fragment. The benzimidazole rings (1, 2) are mutually twisted by 105.1° and by 137.6 and 135.0°, respectively, relative to the central benzene ring (3), and the copper center is displaced by 0.214(8) Å from the mean, equatorial CuN_2OCl plane toward the apical DMF. The copper centers are separated by 8.805(3) Å, which is significantly longer than in the 2:2 fragment.

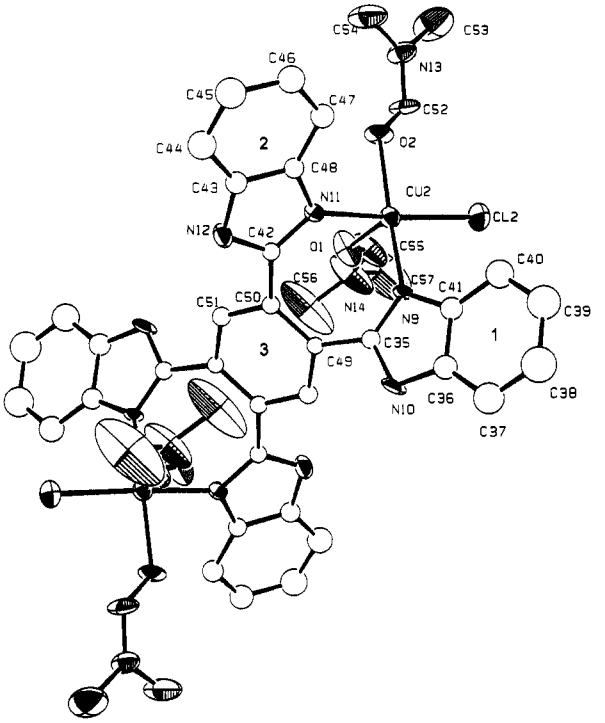

Figure 3. Perspective view of 2:1 nonmetallacyclic cation $[Cu_2(BTBI)Cl_2(DMF)_4)_2]^{2+}$ in **II**.

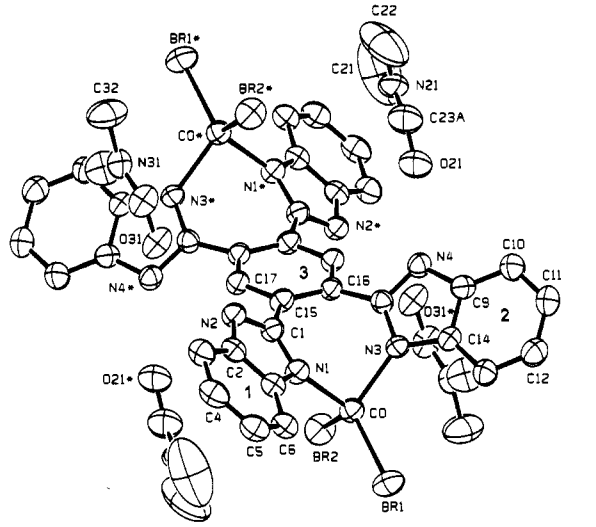

Figure 4. Structural representation of $[Co_2(BTBI)Br_4] \cdot 4DMF$ (**XI**) with hydrogen atoms omitted (40% probability thermal ellipsoids).

Description of the Structure of $[Co_2(BTBI)Br_4] \cdot 4DMF$ (XI). The structure of **XI** is shown in Figure 4, and bond lengths and angles relevant to the cobalt coordination spheres are listed in Table 5. The molecule is centrosymmetric, with the center of inversion at the center of the central benzene ring of the BTBI ligand. Each cobalt center is bound to two nitrogen atoms and two bromine atoms on each side of the ligand. The stereochemistry

Table 5. Intramolecular Distances (Å) and Angles (deg) Relevant to the Cobalt Coordination Spheres in $[Co_2(BTBI)Br_4]\cdot 4DMF$ (**XI**)

Co–Br(1)	2.367(2)	Co–Br(2)	2.363(2)
Co–N(1)	2.016(6)	Co–N(3)	2.004(7)
Co–Co′	8.652(3)		
Br(1)–Co–Br(2)	113.15(7)	Br(1)–Co–N(1)	114.6(2)
Br(1)–Co–N(3)	114.6(2)	Br(2)–Co–N(1)	110.6(2)
Br(2)–Co–N(3)	110.4(2)	N(1)–Co–N(3)	91.7(3)

at each cobalt center is slightly distorted tetrahedral, with angles at cobalt ranging from 110.4(2)° (Br(2)–Co–N(3)) to 114.6(2)° (Br(1)–Co–N(3)). This contrasts somewhat with the geometry around cobalt in $[Co_2(BTIM)Cl_4]\cdot 2DMF$,[4] where comparable angles fell in the range 96.2(2)–116.8(2)°. The cobalt–nitrogen distances are almost equal (Co–N(1) = 2.016(6) Å, Co–N(3) = 2.004(7) Å) and compare closely with those in $[Co_2(BTIM)Cl_4]\cdot 2DMF$. The cobalt–bromine distances (Co–Br(1) = 2.367(2) Å, Co–Br(2) = 2.363(2) Å) are almost equal and are considered normal. Due to the placement of two benzimidazole groups at the 1- and 2-positions of the benzene ring, seven-membered chelate rings are formed, and as a result, the benzimidazole rings are mutually twisted and are also twisted relative to the central benzene ring (Figure 4) (dihedral angles between least-squares planes: 1–2, 66.39°; 1–3, 38.84°; 2–3, 45.04°). The overall twisting of the benzimidazole rings relative to the central benzene is significantly smaller in **XI** than in $[Co_2(BTIM)Cl_4]\cdot 2DMF$. However this may be due, in part, to the presence of different halogens in these two compounds. The DMF solvent molecules are hydrogen-bonded via O(21) and O(31) to hydrogen atoms attached to the benzmidazole nitrogen atoms N(4) and N(2), respectively (O(21)–N(4) = 2.73 (1) Å, O(31)–N(2) = 2.73(1) Å). One of the DMF molecules (O(21)) is disordered. The two cobalt centers are separated by a long distance of 8.652(3) Å, which is comparable to that observed in an analogous cobalt(II) complex of the BTIM ligand (Co–Co = 8.736(3) Å).[4]

Spectral, Structural, and Magnetic Properties. In the infrared spectra of these complexes, strong absorptions occurring in the region 1638–1682 cm^{-1} (Table 6) are associated with the C=O stretch of DMF molecules. Bands in the range 1638–1648 cm^{-1} are assigned to coordinated DMF, while bands at higher energy are associated with uncoordinated, lattice DMF molecules, some of which are involved in hydrogen bonding. The presence of two weak absorptions at 1743 and 1731 cm^{-1} ($\nu_1 + \nu_4$ combination bands) for **V** are indicative of monodentate coordination of the nitrates.[22] The splitting of the trifluoromethanesulfonate bands (1170–1286 cm^{-1}; 517–527 cm^{-1}) for **VIII**, associated with the ν_4(E) and ν_5(E) modes of vibration, respectively, suggests that the symmetry of the SO_3 group has been lowered to C_s, indicative of coordinated monodentate triflate.[23] The triflate bands for **IX** are somewhat different but are still of low symmetry (Table 6). However, the presence of coordinated DMF and the likely five-coordinate structure for this compound suggests that the triflate groups are not ligands but are probably involved in hydrogen bonding with lattice water molecules. The band at 2068 cm^{-1} for **XII** indicates the presence of coordinated isothiocyanate. A general similarity in the infrared spectra of **X**–**XII** suggests similar structures for these compounds.

The 2:2 complexes **VII** and **IX** apparently have metallacyclic structures similar to that of the 2:2 cation found in **II**. These species exhibit a single solid-state electronic spectral band at 580 nm, indicative of square-pyramidal copper(II) centers. An analogous perchlorate complex, $[Cu_2(BTBI)_2(DMF)_2](ClO_4)_4\cdot x$DMF, has been examined structurally, but a poor data set and the difficulty of locating a large number of lattice DMF molecules precluded a successful refinement of the structure. However, the main structural fragment clearly shows a 2:2 metallacyclic cation with square-pyramidal copper centers, involving four nitrogen atoms in the equatorial plane and axially bound DMF. This is supported by a strong infrared band at 1087 cm^{-1}, due to ionic perchlorate, and bands at 1641 and 1669 cm^{-1}, due to coordinated and lattice DMF.[21] This compound has a strong, broad visible band at 610 nm, comparable with those for **VII** and **IX**, thus suggesting similar structures.

2:1 complex copper cations are found in compounds **I**, **II**, **IV**–**VI**, and **VIII** and are generally characterized by longer wavelength absorption compared to that of the 2:2 species. The dominant copper ion stereochemistry for these species is likely to be square-pyramidal, as is found in **II**, but quantifying the fine details of the ligand environment is difficult. **I** and **II** appear to contain different 2:1 cations, with possible coordination of four chlorides in **I**. In the far-infrared region, bands at 319, 298 cm^{-1} (**I**), 256, 237 cm^{-1} (**III**), 333, 321 cm^{-1} (**X**), and 257, 230 cm^{-1} (**XI**) are assigned to metal–halogen stretch, while bands observed in the range 284–334 cm^{-1} for **XII** are assigned to metal–nitrogen stretch. The similarity in visible absorption between **II** and **IV** suggests a similar mixed-stoichiometry complex in **IV**, and characteristic long-wavelength absorption at 1100 nm for **III** strongly supports the presence of the $CuBr_4^{2-}$ anion. **VI** contains coordinated and noncoordinated DMF and ionic tetrafluoroborate, and on the reasonable assumption that the copper centers are five-coordinate, three water molecules and three DMF molecules appear to be coordinated, which is further supported by a sharp absorption at 3557 cm^{-1}, associated with coordinated water.

The solid-state mull transmittance spectra (Table 6) of compounds **X**–**XII** are characterized by the presence of two major absorption regions in the visible and near-infrared (<1700 nm) regions, clearly resolved into three components in most cases, and are associated with components of the ν_3 and ν_2 transitions, respectively, in tetrahedral cobalt(II) centers, which arise through lowering of the symmetry to C_{2v}. Three other relatively weak, low-energy components can also be observed for these compounds in the range 1900–2300 nm, which appear to be d–d in origin, and are associated with similar components of the ν_1 transition ($^4T_1(P) \leftarrow {}^4A_2(\nu_3)$; $^4T_1(F) \leftarrow {}^4A_2(\nu_2)$; $^4T_2 \leftarrow {}^4A_2(\nu_1)$). The observation of these bands, at such low energy, in somewhat unusual in the solid state and is an indication of the sensitivity of the spectrometer. $10Dq$ values have been calculated using the average band energies of the components of the ν_2 and ν_3 transitions, and as might be expected, the order of $10Dq$ [Br (4020 cm^{-1}) < Cl (4220 cm^{-1}) < NCS (4640 cm^{-1})] reflects the ligand field strengths of the coordinated anions. It is reasonable to assume that **X** and **XII** have similar pseudotetrahedral structures. The absorption energies for **X**–**XII** compare closely with those of analogous dinuclear complexes of BTIM (1,2,4,5-tetrakis(4,5-dihydroimidazol-2-yl)benzene) and mononuclear complexes involving the ligands 1,2-bis(4,5-dihydroimidazol-2-yl)benzene and 1,2-bis(6-methylbenzimidazol-2-yl)benzene, all of which have similar donor groups producing equivalent, seven-membered chelate rings.[4,24,25]

Room-temperature magnetic moments for compounds **I**–**IX** are all in excess of the spin-only value for the copper(II) ion (Table 6), which suggests that any spin–spin coupling in these systems is likely to be weak or nonexistent. Because of the dinuclear nature of these complexes, with an intervening aromatic π-system between the distant metal centers similar to that in the 2:2 BTIM complexes, which were shown to have weak antiferromagnetic exchange ($-2J < 2$ cm^{-1}),[3] significant spin exchange was not anticipated for the 2:2 complexes of BTBI. Consequently,

(22) Lever, A. B. P.; Mantovani, E.; Ramaswamy, B. S. *Can. J. Chem.* **1971**, *49*, 1957.
(23) Castro, I.; Faus, J.; Julve, M.; Bois, C.; Real, J. A.; Lloret, F. J. *J. Chem. Soc., Dalton Trans.* **1992**, 47.
(24) Lever, A. B. P.; Ramaswamy, B. S.; Simonsen, S. H.; Thompson, L. K. *Can. J. Chem.* **1970**, *48*, 3076.
(25) Wellon, G. C.; Bautista, D. V.; Thompson, L. K.; Hartstock, F. W. *Inorg. Chim. Acta* **1983**, *75*, 271.

Table 6. Infrared, Electronic, and Magnetic Data

complex	color	infrared data (cm^{-1})	electronic data (nm)[a]	room-temp μ_{eff} (μ_B)
$[Cu_2(BTBI)Cl_4(DMF)_2]\cdot DMF\cdot H_2O$ (I)	dark green	3442, 1645, 319, 309, 298, 289	[710], 625, [400]	1.88
$[Cu_2(BTBI)_2Cl_2][Cu_2(BTBI)Cl_2(DMF)_4]Cl_4\cdot 12DMF$ (II)	green	1682, 1665, 1652, 1638	700, 360	1.93
$[Cu_2(BTBI)Br_2(DMF)_2(H_2O)_2][CuBr_4]\cdot 2H_2O$ (III)	brown	3466, 1643, 300, 287, 256, 237	1100, 600, 530, 355	1.78
$[Cu_2(BTBI)_2Br_2][Cu_2(BTBI)Br_2(DMF)_4]Br_4\cdot 6DMF\cdot 4H_2O$ (IV)	bright green	3382, 1664, 1651	700, 370	1.85
$[Cu_2(BTBI)(DMF)_2(NO_3)_4]\cdot 2DMF\cdot 3H_2O$ (V)	blue-green	1743, 1731, 1672, 1643, 361, 317, 296	[710], 625, 360	1.89[b]
$[Cu_2(BTBI)(DMF)_3(H_2O)_3](BF_4)_4\cdot DMF$ (VI)	blue-green	3557, 1667, 1648, 1089, 1053, 304, 289	710, [640], 350	1.92[b]
$[Cu_2(BTBI)_2(DMF)_2](BF_4)_4\cdot 2DMF\cdot 2H_2O$ (VII)	green-blue	3520, 1668, 1643	580	1.86
$[Cu_2(BTBI)(DMF)_2(CF_3SO_3)_4]2H_2O\cdot 2DMF$ (VIII)	blue-green	3494, 1662, 1643, 1286, 1245, 1226, 1170, 527, 517, 351, 308, 288	695, 645, 385	2.06
$[Cu_2(BTBI)_2(DMF)_2](CF_3SO_3)_4\cdot DMF\cdot 5H_2O$ (IX)	green-blue	3467, 1666, 1641, 1294, 1239, 526, 516	580, 380	1.85
$[Co_2(BTBI)Cl_4]\cdot 2DMF\cdot 0.5H_2O$ (X)	blue	3389, 1649, 333, 321, 313, 298	2270, 2140, 1950, 1650, 1370, 1040, 650, 615, 585, 360	4.47
$[Co_2(BTBI)Br_4]\cdot 2DMF$ (XI)	blue	1652, 301, 280, 257, 230	2280, 2120, 1920, 1700, 1440, 1060, 660, 625, 590, 370	4.74
$[Co_2(BTBI)(NCS)_4]\cdot 2DMF\cdot 3H_2O$ (XII)	blue	3400, 2068, 1652, 334, 315, 296, 284	2300, 2100, 1925, 1550, 1255, 970, 625, 575, 350	4.74

[a] Mull transmittance ([ ] = shoulder). [b] V: $-2J = 0.56(6)$ cm^{-1}, $g = 2.199(4)$. VI: $-2J = 0.89(5)$ cm^{-1}, $g = 2.234(4)$. (Data were fitted to eqs 2 and 3).

variable-temperature magnetic studies were carried out on powdered samples of the 2:1 derivatives V and VI in the temperature range 4–300 K to see whether a significant change in overall structure had any major effect on spin coupling. The variable-temperature susceptibility data were fitted to the Bleaney–Bowers expression (eq 1)[26]

$$\chi_m = (N\beta^2g^2/3kT)[1 + {}^1/_3\exp(-2J/kT)]^{-1} + N\alpha \quad (1)$$

using the isotropic (Heisenberg) exchange Hamiltonian ($H = -2JS_1\cdot S_2$) for two interacting $S = {}^1/_2$ centers (χ_m is expressed per mole of copper atoms, and $N\alpha$ is the temperature-independent paramagnetism, set at 95×10^{-6} cgsu). A nonlinear regression analysis[27] was employed, with g and J as variables, giving $g = 2.237(4)$ and $-2J = 1.5(2)$ cm^{-1} (a comparable analysis was obtained for VI). Since the singlet–triplet splitting in both cases is likely to be comparable with the Zeeman energy, $g\beta H$, the data were also fitted to the magnetization expression (eqs 2 and 3).[28,29]

$$M = Ng\beta(\sinh(g\beta H/kT))/(\exp(-2J/kT) + 2\cosh(g\beta H/kT) + 1) \quad (2)$$

$$\chi_m = M/H + N\alpha \quad (3)$$

Values of g and $-2J$ obtained from this analysis (Table 6) are slightly different from those obtained from the Bleaney–Bowers analysis, but the data fits are much better. A plot of χ_m versus T for V and the best fit theoretical line, based on this analysis, are given in supplementary Figure S1. Very weak antiferromagnetic exchange exists between the two copper centers in both compounds. It is reasonable to assume that, in the other copper(II) complexes of BTBI, very weak antiferromagnetic coupling also exists between the copper centers.

The room-temperature magnetic moments (Table 6) for **X**–**XII** (4.47–4.74 μ_B/Co) are typical of pseudotetrahedral cobalt(II) complexes. Variable-temperature magnetic data were collected for **XI** and **XII** in the temperature range 5–300 K. Reciprocal susceptibility versus temperature plots for both **XI** and **XII** are essentially linear, and a linear regression of the data reveals a small negative temperature intercept (−1.9 K) for **XI** and a small positive temperature intercept for **XII** (+0.86 K). For the bromo complex, the negative value might signal antiferromagnetic coupling. The magnetic data for **XI** were fitted to an exchange equation derived from the Van Vleck expression[30] for an isotropic, Heisenberg $S = {}^3/_2, {}^3/_2$ pair. A very small negative J value ($-J = 0.29(1)$ cm^{-1}; $g = 2.524(4)$) was obtained. Such a small value cannot be considered meaningful, and the slight drop in magnetic moment at low temperature should perhaps be attributed to zero-field-splitting effects. The magnetic moment remains essentially constant in the range 25–300 K (approximately 4.5 μ_B), dropping to 4 μ_B at about 5 K. The case for the isothiocyanate complex **XII** is different. The small positive temperature intercept ($1/\chi$ vs T) suggests possible ferromagnetic coupling. The magnetic moment rises steadily from 4.74 μ_B at 299 K to a maximum of 4.91 μ_B at 17.5 K and then drops to 4.56 μ_B at 4.9 K. Fitting the susceptibility data to an isotropic $S = {}^3/_2, {}^3/_2$ Heisenberg expression over the entire temperature range gave $J = 57(5)$ cm^{-1} ($g = 2.035(6)$). Even considering the inherent problems of establishing exchange integrals with accuracy for ferromagnetically coupled systems, the fact that J is positive in this case is somewhat surprising. The spectral similarities between the three pseudotetrahedral cobalt(II) complexes suggest nothing unusual in the structure of this species, and it is expected to have a structure similar to that of **VII**. However, in the absence of structural data, comments on the origin of this coupling are perhaps inappropriate. The lack of perceptible coupling for **XI** is consistent with the weak coupling observed for the copper complexes.[3]

The powdered X-band ESR spectra of complex I recorded at both 295 and 77 K are essentially the same and typical of an axial species with $g_\parallel = 2.22$ and $g_\perp = 2.06$ (77 K). The solid-state spectrum of **II** at 295 K (Figure 5) is very reminiscent of the solid-state spectrum of $[Cu_2(BTIM)_2(H_2O)_2](BPh_4)_2\cdot 6H_2O$.[3] Seven well-resolved hyperfine lines are observed in the parallel region at room temperature with an average splitting of 72.5 G. At 77 K, six lines are visible with an average splitting of 76.8 G. These spectral features in the parallel region are typical of a dinuclear system with a very weak exchange interaction.[31–34] No discernible hyperfine lines are observed on the high-field side of the $g_\perp$ transition, as might be expected, but due to possible small zero-field splitting they may be buried under this fairly broad signal. The DMF solution spectrum at room temperature is not informative, appearing as a rather broad signal with features at

(26) Bleaney, B.; Bowers, K. D. *Proc. R. Soc. London, A* **1952**, *214*, 451.
(27) Duggleby, R. G. *Anal. Biochem.* **1981**, *110*, 9.
(28) Myers, B. E.; Berger, L.; Friedberg, S. *J. Appl. Phys.* **1969**, *40*, 1149.
(29) Marsh, W. E.; Patel, K. C.; Hatfield, W. E.; Hodgson, D. J. *Inorg. Chem.* **1983**, *22*, 511.
(30) Van Vleck, J. H. *The Theory of Electric and Magnetic Susceptibilities*; Oxford University Press: London, 1932.
(31) Yokoi, H. *Chem. Lett.* **1973**, 1023.
(32) Felthouse, T. R.; Laskowski, E. J.; Hendrickson, D. N. *Inorg. Chem.* **1977**, *16*, 1077.
(33) Felthouse, T. R.; Hendrickson, D. N. *Inorg. Chem.* **1978**, *17*, 444.
(34) Haddad, M. S.; Hendrickson, D. N. *Inorg. Chem.* **1978**, *17*, 2622.

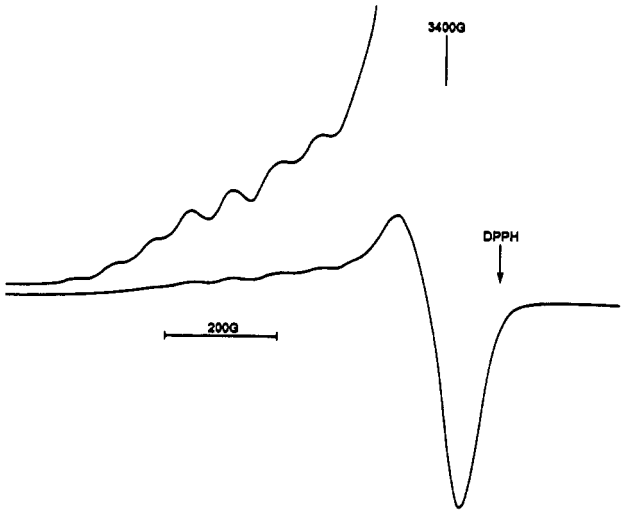

Figure 5. X-Band ESR spectrum for $[Cu_2(BTBI)_2Cl_2][Cu_2(BTBI)Cl_2(DMF)_4]Cl_4 \cdot 12DMF$ (**II**) (solid state) at room temperature (9.76 GHz).

$g = 2.23$ and $g = 2.10$. Cooling to 77 K did not provide any significant resolution in the parallel region, typical of the BTIM systems.[3] Since two different dinuclear species are present in **II**, the question arises as to which species is responsible for the spectrum. The same characteristic splitting pattern was observed for all of the 2:2 complexes in the solid state, including the structurally characterized complex $[Cu_2(BTBI)_2(DMF)_2](ClO_4)_4 \cdot x$DMF,[21] which involves the familiar 2:2 metallacyclic five-coordinate cation. A typical room-temperature spectrum, for compound **VII**, is illustrated in supplementary Figure S2. This suggests that the ESR spectrum for **II** is dominated by the 2:2 metallacyclic cation. **III** has a very broad featureless isotropic signal both at 295 and 77 K ($g_0 = 2.14$), which can be associated with the $CuBr_4^{2-}$ anion, but the recrystallized sample **IV** has the same characteristic seven-line spectrum observed for **II** and the 2:2 species (average splitting 72.1 G; 295 K).

V has a typical axial solid-state spectrum at both 295 and 77 K ($g_\parallel = 2.31$, $g_\perp = 2.15$) associated with the 2:1 cation, but a recrystallized sample, which is green-blue, displays a seven-line spectrum (average splitting 79.2 G; 295 K), indicative of disproportionation to produce a 2:2 derivative. Solid-state spectra for **VI** and **VIII** are identical and do not exhibit the axial features found for **I** and **V**, but rather show what can be described as an asymmetric splitting in the $g_\parallel$ region, similar to the 2:2 pattern, but with only six discernible lines with an average splitting of about 73 G (room temperature). An identical splitting pattern was observed for the parent 2:1 perchlorate complex. However, the recrystallized species **VII** and **IX** (and also $[Cu_2(BTBI)_2(DMF)_2](ClO_4)_4 \cdot x$DMF; average splitting 77.1 G (room temperature)) show the normal seven-line pattern in the solid state (average splitting 79.1 G (room temperature) for **VII**; average splitting 82.5 G (room temperature) for **IX**) expected for the 2:2 species.

The room-temperature and 77 K solid-state spectra of all the compounds containing 2:2 cations exhibit essentially identical spectra at both temperatures. Such a situation is unusual and indicates that the dinuclear species are well separated in the lattice and that only weak intradinuclear coupling effects are at play. Cooling to 77 K does not cause any significant change, suggesting no interdimer associations at low temperature. In no instances were $\Delta M_s = \pm 2$ transitions observed for the 2:1 or 2:2 derivatives.

Acknowledgment. We thank the Natural Sciences and Engineering Research Council of Canada for financial support of this study.

Supplementary Material Available: Tables listing detailed crystallographic data, hydrogen atom positional parameters, anisotropic thermal parameters, bond lengths and angles, and least-squares planes, a plot of χ_m versus T for **V**, and the solid-state X-band ESR spectrum (room temperature) for **VII** (45 pages). Ordering information is given on any current masthead page.